Generalized Background-Field Method

Y.J. Feng* and C.S. Lam[†]

Department of Physics, McGill University, 3600 University St., Montreal, P.Q., Canada H3A 2T8

Abstract

The graphical method discussed previously can be used to create new gauges not reachable by the path-integral formalism. By this means a new gauge is designed for more efficient two-loop QCD calculations. It is related to but simpler than the ordinary background-field gauge, in that even the triple-gluon vertices for internal lines contain only four terms, not the usual six. This reduction simplifies the calculation inspite of the necessity to include other vertices for compensation. Like the ordinary background-field gauge, this generalized background-field gauge also preserves gauge invariance of the external particles. As a check of the result and an illustration for the reduction in labour, an explicit calculation of the two-loop QCD β -function is carried out in this new gauge. It results in a saving of 45% of computation compared to the ordinary background-field gauge.

1 Introduction

Physical processes in QCD are gauge independent but unfortunately individual Feynman diagrams are not. For that reason calculations may be greatly simplified with the choice of a convenient gauge, so as to minimize the presence of gauge-dependent terms in the intermediate steps. The background-field (BF) gauge [1] is one such gauge, partly because of its gauge-invariant property with respect to the external lines. The pinching technique [2, 3] used to simplify calculations is also known to be related to this gauge [4, 5].

The purpose of this paper is to discuss a graphical method for designing other convenient gauges. We start by pointing out the advantage and the flexibility of the graphical method over the conventional path-integral or operator technique.

The gluon propagator $g^{\mu\nu}/p^2$ will be used throughout, thus by a gauge choice we just mean the choice of vertices in making calculations. The BF vertices are different from the ordinary vertices in that its triple-gluon (3g) vertex makes a distinction between internal and external gluon lines, with the latter indicated graphically by an arrow (see Fig. 7(a) of the Appendix) and analytically possessing only four (see eq. (9) of the Appendix) rather than the usual six (eq. (17) and Fig. 7(i)) terms. The Gervais-Neveu gauge [6] would be another possible gauge choice in this sense.

In the usual approach, gauge choice is implemented by a gauge-fixing term in the path integral. In the BF gauge, for example, this term for the quantized Yang-Mills field Q is

given by $\partial \cdot Q + g[A, Q]$, with A being an external classical Yang-Mills potential. The presence of A is the reason why external lines play a special role in the BF gauge.

In a previous publication [5] we have demonstrated how this and other gauge choices can be obtained in a graphical method, which we will summarize and extend in Sec. 2. Similar techniques have also been employed elsewhere [7, 8]. Essentially, in the graphical language, the fundamental difference between one gauge and another lies in their 3g vertices, which differ from one another by a combination of gradient terms. To compensate for this difference changes will have to be made in other vertices as well, changes that can be computed using the graphical method. With this technique it is possible to make different changes on different vertices, each leading to a different compensation. In contrast, a gauge-fixing term in the path-integral or the operator formalism does not possess this flexibility; whatever changes made to one vertex must be made on other identical vertices. Hence we can design newer and simpler gauges using the graphical method that cannot be obtained using the path-integral method. The generalized background-field [GBF] gauge discussed later is such a gauge, and we are also considering another one that is related to the Gervais-Neveu gauge [9].

This paper is organized as follows. In Sec. 2, we review and extend the graphical procedure for creating new gauges [5]. The GBF gauge will be defined in Sec. 3, and the computation of the 2-loop β -function using this new gauge is presented in Sec. 4, with a conclusion in Sec. 5.

2 Graphical Procedure for the Creation of New Gauges

To discuss gauge invariance graphically, it is convenient to use the Chan-Paton color factors [10] and color-oriented diagrams [11, 12].

In the absence of quarks, the Chan-Paton color factors are given by the traces of products of the color matrices T^a , and the products of such traces. In the presence of quarks, ordered products of the color matrices T^a also enter.

Diagrammatic rules can be designed to compute the spacetime amplitudes for each of these color factors, by using *color-oriented diagrams*. The propagators of the color-oriented diagrams are the ordinary propagators; their vertices are different but can be derived from the vertices of Feynman diagrams. For one thing, color factors are no longer present in the vertices of the color-oriented diagrams. For another, the clockwise orientation of the lines emerging from each vertex is fixed in the color-oriented diagrams (hence the name). These color-oriented vertices are given in eqs (2.1) to (2.4) as well as Fig. 1 of Ref. [9] in the Feynman gauge.

In what follows, when we talk about diagrams we mean the color-oriented diagrams, and when we talk about vertices we always refer to these color-oriented vertices.

The graphical rules for gauge transformation of color-oriented diagrams have been discussed before [5]. Using these rules we can create new gauges not reachable in the path-integral formalism. By new gauges in this paper we shall mean new vertex factors; the propagators used here will always be the usual Feynman-gauge propagators.

To create a new gauge B from an existing gauge A, we start by subtracting appropriate

combinations of gradient terms from the triple-gluon (3g) vertices $\Gamma_{\alpha\beta\gamma}(p_1, p_2, p_3)$ of gauge A, viz., terms proportional to $(p_1)_{\alpha}$, $(p_2)_{\beta}$, and $(p_3)_{\gamma}$. Such a gradient term will be denoted graphically by a cross (×) on the appropriate gluon line.

To maintain gauge invariance and the same physical scattering amplitudes, other vertices must also be altered and/or created to compensate for this change. Using graphical methods [5] they can be computed in the following way.

A gradient term on a 3g vertex becomes a divergence on the subsequent vertex. To find out the effect of this change on the 3g vertex, we need to know the divergence of every vertex possessing a gluon line in the original gauge A.

If A consists of the vertices of the ordinary Feynman gauge given by eqs. (2.1) to (2.4) and Fig. 1 of Ref. [5], then these divergences are given by eqs. (2.5) to (2.8) and expressed graphically in Figs. 2 to 5 of that paper.

If A consists of the vertices of the background-field (BF) gauge given by eqs. (2.1) to (2.4), as well as (4.1) to (4.7) of Ref. [5], and graphically Figs. 1 and 18 of that paper, then these divergences can be similarly computed. The BF vertices are repeated here in the Appendix, eqs. (7) to (17), and graphically in Figs. 7(a) to (k). The result of the divergence computation can be found in Figs. 8 to 13.

The next step is to combine the right-hand side of the divergence relations from different diagrams. On account of local gauge invariance, many of these terms add up to cancel one another. Starting from the Feynman gauge, these cancellation relations can be found in Figs. 7 to 16 of Ref. [5]. Starting from the BF gauge, similar relations can be worked out and they are shown in Figs. 14 to 17 in the Appendix of this paper.

This general scheme works in QED as well as QCD. What makes them different is the presence of ghost lines in the latter. Among other things, it gives rise to the presence of propagating diagrams in the divergence relation of 3g and possibly 4g vertices. These are diagrams in which two of the gluon lines are replaced by ghost lines (we call them wandering ghost lines), and the divergence 'cross' at the beginning of a line is moved to the end of the other line, as in Figs. 3(d) and 3(e) of Ref. [9] for the Feynman gauge, and Figs. 8(d) and 8(e) of this paper for the BF gauge. Via these diagrams, the divergence 'cross' propagates along the diagram, dragging behind it the wandering ghost line. It is the presence of these diagrams that makes the Slavnov-Taylor identity in QCD different from the Ward-Takahashi identity in QED.

If the cross propagates in a closed loop to return to its original position, then local gauge compensation will be upset, thus resulting in additional terms or vertices with two ghost lines. For example, if gauge A is Feynman and gauge B is BF, then this change is given by Fig. 20 of Ref. [5].

We started with the gradient change of a *single* 3g vertex in gauge A for every diagram, as described above, and considered the local cancellations and the new ghost vertices thus created for gauge B. Having converted one vertex this way, we are now ready to convert a second 3g vertex from gauge A to gauge B. Unless the second vertex is adjacent to the first, the same argument holds and the net change of the second vertex is identical to that of the first. If they are adjacent, additional changes may occur because the first 3g and ghost vertices are already in gauge B, while the second vertex is still in gauge A. Mixing A and

B, local gauge cancellation will generally not occur, thus producing yet other new terms or vertices from this mismatch. In getting from the Feynman gauge to the BF gauge in Ref. [5], for example, this is how the new 4g vertices are obtained through Figs. 37 and 38.

We can continue this way to change *all other* vertices one after another from gauge A to gauge B. In principle, merging three or more adjacent vertices may produce newer vertices still, but this does not happen when we go from the Feynman to the BF gauge, nor from the BF gauge to the GBF gauge as will be discussed in the next section.

3 Generalized Background-Field (GBF) Gauge

In this section we follow the outline of the last section to convert the BF gauge to a new gauge which we shall refer to as the GBF gauge.

In the BF gauge, the 3g vertices involving an external gluon are different from those without it. The former has four terms compared to the latter with six terms. The former is shown in Fig. 7(a) of the Appendix, in which the external line is represented by an arrow. The latter is just the usual 3g vertex shown in Fig. 7(i). The aim of the GFB gauge is to convert all 3g vertices to the former type with only four terms, so as to simplify the number of terms present and the algebra of the calculations. It is true that new vertices and diagrams will have to be produced to compensate for this change, but the overall saving turns out to be still substantial. In this paper, we confine ourselves to two-loop diagrams with an arbitrary number of external lines. In fact, we will carry out the explicit calculation only for two external lines but the technique can easily be generalized to an arbitrary number of external lines. With this restriction there are at most two internal 3g vertices in the BF gauge that need be converted into the arrowed type. We will choose the arrows to appear on both ends of the 'middle propagator' as shown in Figs. 6(a) and 6(b) of the next section.

As before, let us make this change first on one of the two internal vertices. The change is identical to what happens when we convert from the Feynman to the BF gauge, so nothing new will be produced. Now we convert the second internal 3g vertex to the arrowed form. Via a series of propagating diagrams, the 'cross' can return to this vertex via two possible routes. Either it comes back via a line without an arrow, or it returns via the arrowed line. The former is identical to what happened before so it produces nothing new. The latter could not happen previously because the arrowed line in the BF gauge is always an external line. Now in the GBF gauge, this new situation produces a new vertex shown in Fig. 1. In addition, adjacent interaction may now take place when the ghost line returns in a loop, and this produces further changes given by Figs. 2 to 4.

The vertices obtained this way for the GBF gauge is summarized in Fig. 5 and eqs. (1)–(6).

$$[5a] = 0 \tag{1}$$

$$[5b] = g^2 g^{\alpha\beta} \tag{2}$$

$$[5c] = g^2 g^{\alpha\beta} \tag{3}$$

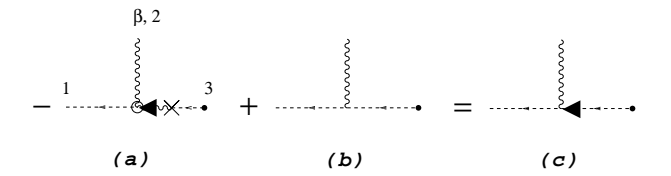


Figure 1: Generation of a ghost vertex in the GBF gauge. The small circle in (a) represents a factor of $g_{\beta\gamma}$, and the cross denotes p_3^{γ} . A dot at the end of a line means that the propagator of the line is included. The propagator of line-3 in (a) is a ghost propagator.

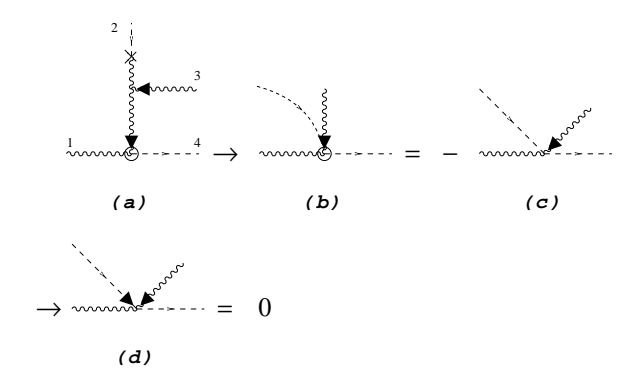


Figure 2: Cancellation of a ghost vertex in the GBF gauge. The cross on line-2 of (a) generates a sliding diagram as shown in (b), which up to a sign is equal to (c), a ghost coupling already exists in the BF gauge. (d) is the summation of (b) and (c). It is zero.

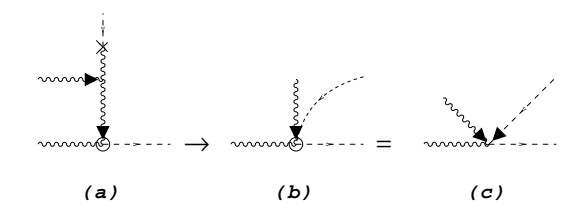


Figure 3: Generation of another ghost vertex in the GBF gauge.

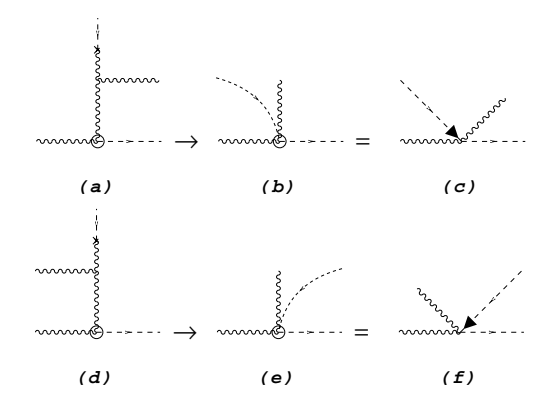


Figure 4: Generation of other ghost vertices in the GBF gauge.

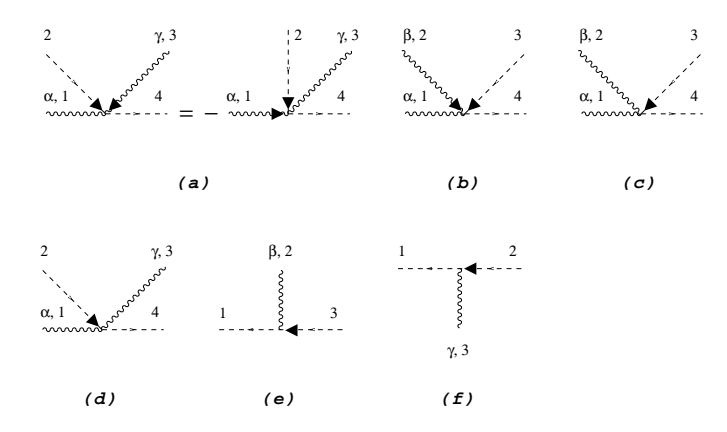


Figure 5: New vertices in GBF gauge. Vertices involving the arrowed ghost lines originates from the internal arrowed gluon lines in the GBF gauge. All the BF gauge vertices in Fig. 7 are still present.

$$[5d] = g^2 g^{\alpha \gamma} \tag{4}$$

$$[5e] = -gp_2^{\beta} \tag{5}$$

$$[5f] = gp_3^{\gamma} \tag{6}$$

4 β -Function at the Two-Loop level

As an illustration, and a check of these new vertex rules, we will calculate the QCD two-loop β function in the GFB gauge. This β -function has previously been done in the Feynman and the BF gauges [13], with considerable savings shown when computed in the BF gauge. We will now show that a further saving of 45% is possible when computed in the GBF gauge.

We choose this example for illustration because it is the simplest at the two-loop level and it can be computed analytically. The disadvantage of this example is that it is not an on-shell process, so the full-fledged simplification of the GBF gauge will not be revealed. Off-shellness gives rise to some *extra* diagrams, which will be absent in an on-shell process. But even so, the saving is still considerable.

The diagrams in the GBF gauge are shown in Fig. 6. There are 26 basic diagrams to be found in Fig. 6(a–z), 12 extra diagrams to be found in Fig. 6(e1–e12), and 3 gauge-fixed renormalization insertion diagrams to be found in Fig. 6(i1, i2, i3). The extra diagrams involve wandering ghost lines sliding to an external end. They will be absent if these external lines were on-shell.

The result of the calculation is summarized in the Table I.

We can compare this with the calculation in the BF gauge [13]. Although we have more diagrams in the GBF gauge, the total number of terms to be computed is less. In the GBF gauge, there are totally 728 terms, while in the BF gauge there are 1320 terms. Therefore, a 45% of computational labor is saved by using the GBF gauge. Using $Mathematica^R$ to compute, we need 150 seconds for the GBF gauge, and 260 for the BF gauge. For on-shell process, because of the absence of the extra diagrams, the saving of the GBF gauge will be greater and can be expected to be approximately 50 percent.

Graph	$g^{\mu u} p^2$		$p^\mu p^ u$	
	$\frac{1}{\epsilon^2}$	1	$\frac{1}{\epsilon^2}$	<u>1</u>
a	11/3	$(54 - 22\rho)/3$	-11/3	$-(56-22\rho)/3$
b	10/3	$(52-20\rho)/3$	-10/3	$-(53-20\rho)/3$
c	-1	0	0	0
d, p	-1/2	$-(3-2\rho)/2$	1/2	$(5-2\rho)/2$
e, k	5/24	$(65 - 20\rho)/48$	-5/24	$-(33-10\rho)/24$
$_{\mathrm{f,j}}$	-1/8	$-(9-4\rho)/16$	1/8	$(9-4\rho)/16$
g,m	1/6	$(13 - 4\rho)/12$	-1/6	$-(3-\rho)/3$
h,i	-5/48	$(-41 + 20\rho)/96$	5/48	$(45 - 20\rho)/96$
l	1/6	$(19 - 4\rho)/12$	-1/6	$-(15-4\rho)/12$
n,o	1/24	$(13 - 4\rho)/48$	-1/24	$-(3-\rho)/12$
q	0	1/2	0	0
r,s,t,u	-1/8	$-(13-4\rho)/16$	1/8	$(9-4\rho)/16$
v,w	-1/48	$-(13-4\rho)/96$	1/48	$(9-4\rho)/96$
x,y	0	0	0	0
Z	-6	$-(24-12\rho)$	6	$(24 - 12\rho)$
e1	5/8	$(33 - 20\rho)/16$	0	0
e2	-9/16	$-(217-36\rho)/32$	0	9/2
e3	1/2	$(5-2\rho)/2$	0	0
e4	-9/16	$-(73-36\rho)/32$	0	0
e5	0	-1/8	0	0
e6	-1/8	$-(9-4\rho)/16$	0	0
e7	-1/8	$-(25-4\rho)/16$	0	1/4
e8	1/4	$(5-2\rho)/4$	0	0
e9	-1/8	$-(13-4\rho)/16$	0	0
e10	-3/16	$-(27-12\rho)/32$	0	0
e11	-3/16	$-(75-12\rho)/32$	0	3/4
e12	1/2	$(5-2\rho)/2$	0	0
i1	25/9	$(230 - 75\rho)/27$	-25/9	$-(230-75\rho)/27$
i2,i3	-25/18	$-(140-75\rho)/54$	25/18	$(140 - 75\rho)/54$
Total	0	17/3	0	-17/3

Table I: The result of two-loop β -function in the GBF gauge. ρ is the same parameter as used in Ref. 13.

5 Conclusion

We have demonstrated the power of the graphical rules in making individual gauge changes on vertices. An operator method or a path-integral method must treat all the vertices the same way so this individual flexibility is lost. This method is illustrated by the creation of the GBF gauge from the BF gauge. GBF gauge maintains the gauge-invariant property of

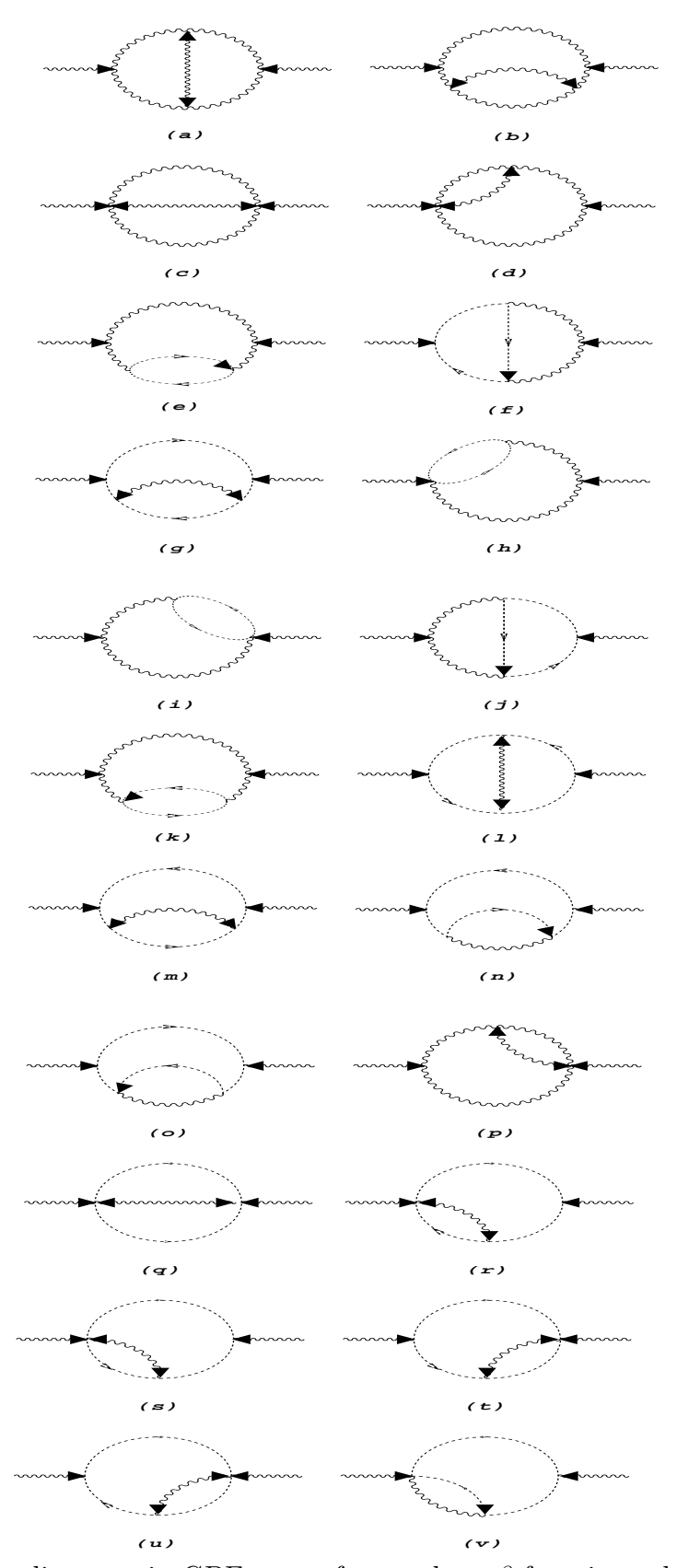


Figure 6: Feynman diagrams in GBF gauge for two-loop β -function calculation of QCD.

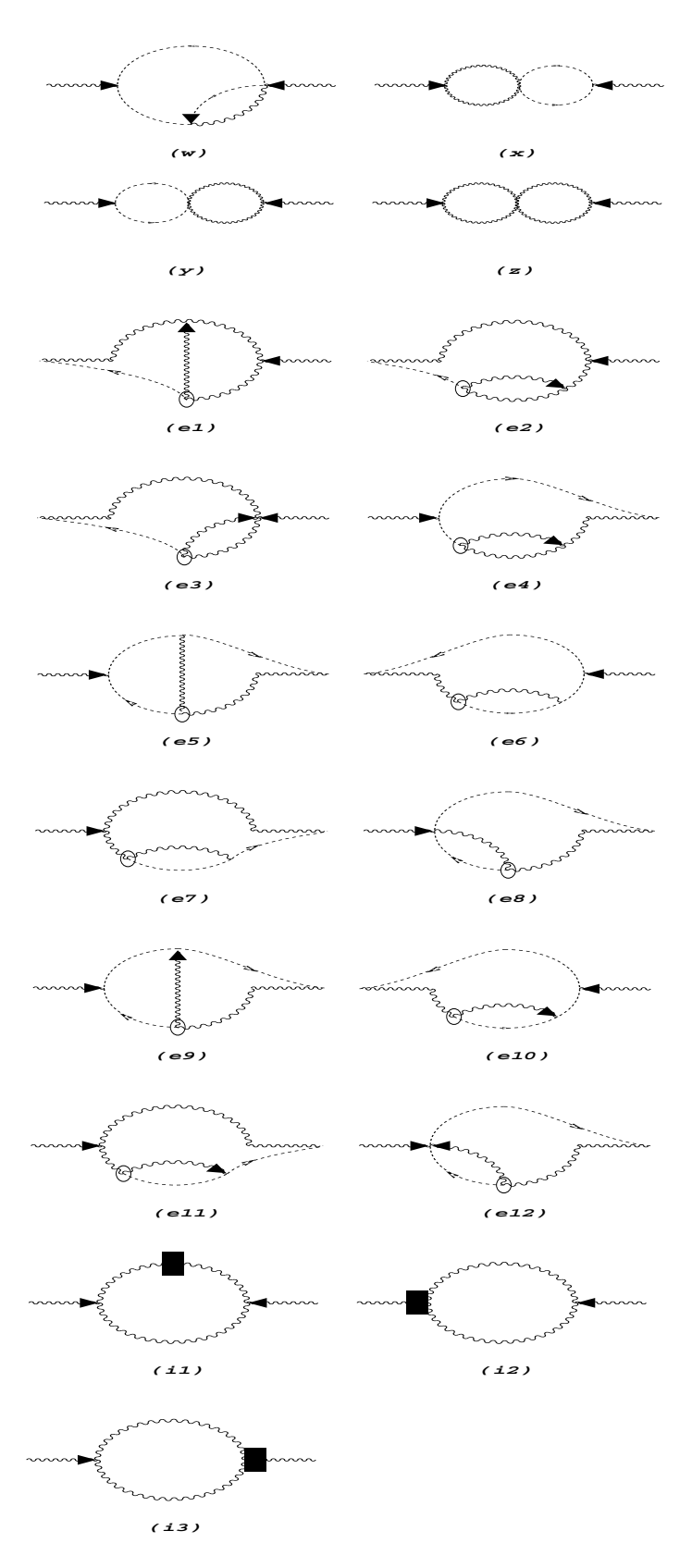


Figure 6: (continued)

the ordinary BF gauge with respect to the external lines, and preserves the simple Ward-Takahashi identity when divergences are taken on them. It also contains less terms than the BF gauge in actual calculations. The saving for the two-loop QCD β -function we gave is 45%, and more can be expected for on-shell processes.

The graphical method is not limited to this example nor this gauge. We can for example change the internal 3g vertices into the 3g vertices of the Gervais-Neveu gauge [6], with even greater saving [9].

Acknowledgements 6

This research was supported in part by the Natural Science and Engineering Research Council of Canada and by the Québec Department of Education. Y.J.F. acknowledges the support of the Carl Reinhardt Major Foundation.

Divergence and cancellation relations in the BF gauge Α

The color-oriented vertices of QCD in the BF gauge are summarized in Fig. 7. We use wavy line for gluon, dotted line for ghost. The arrowed line is an external line. All propagators in this paper are chosen to be in the Feynman gauge, so we have $-1/p^2$ and $q^{\alpha\beta}/p^2$ for ghosts and gluons respectively.

Analytically, the vertices shown in Fig. 7 are associated with the following vertex factors

$$[7a] = g \left[g_{\gamma\alpha}(p_3 - p_1)_{\beta} - 2g_{\alpha\beta}(p_2)_{\gamma} + 2g_{\beta\gamma}(p_2)_{\alpha} \right], \tag{7}$$

$$[7b] = g (p_1 - p_3)_{\beta} , \qquad (8)$$

$$[7c] = g^2 \left[-g_{\beta\gamma}g_{\alpha\delta} - 2g_{\alpha\beta}g_{\gamma\delta} + 2g_{\alpha\gamma}g_{\beta\delta} \right], \tag{9}$$

$$[7d] = -2g^2 g_{\beta\gamma}g_{\alpha\delta} , \qquad (10)$$

$$[7e] = g^2 g_{\beta\gamma} , \qquad (11)$$

$$[7f] = g^2 g_{\beta\gamma} , \qquad (12)$$

$$[7g] = -2g^2 g_{\beta\gamma} , \qquad (13)$$

$$[7h] = g \gamma_{\beta} , \qquad (14)$$

$$[7i] = g[g_{\alpha\beta}(p_1 - p_2)_{\gamma} + g_{\beta\gamma}(p_2 - p_3)_{\alpha} + g_{\gamma\alpha}(p_3 - p_1)_{\beta}], \qquad (15)$$

$$[7j] = g (p_1)_{\beta} ,$$
 (16)

$$[7] = g (p_1)_{\beta},$$

$$[7k] = g^2 \left[2g_{\alpha\gamma}g_{\beta\delta} - g_{\alpha\beta}g_{\gamma\delta} - g_{\alpha\delta}g_{\beta\gamma} \right].$$

$$(10)$$

The divergence and cancellation relations for the BF gauge are summerized below.

A.1Divergence relations

We list below the possibilities when a cross is put on a gluon line without an arrow for any of the vertices found in Fig. 7.

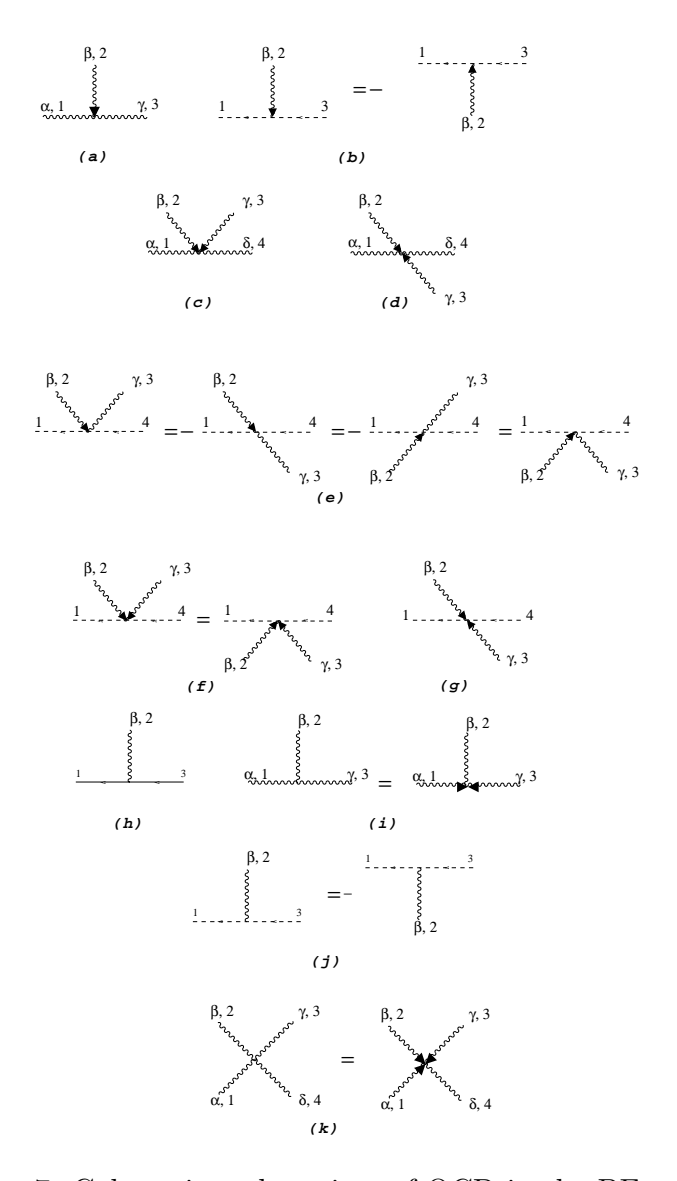


Figure 7: Color-oriented vertices of QCD in the BF gauge.

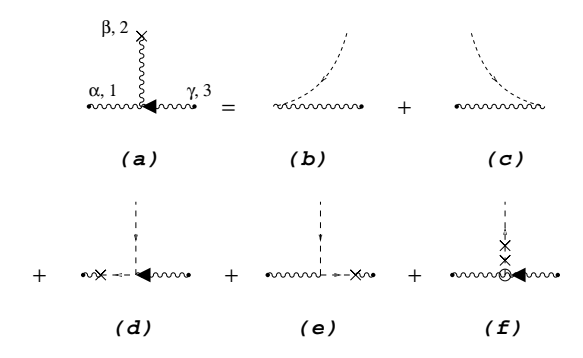


Figure 8: Divergence relation of the triple-gluon vertex (in the BF gauge). (b) and (c) are sliding diagrams. The wandering ghost line tangential to the gluon line means the corresponding gluon propagator has been cancelled. The vertex factor for (b) and (c) is just $gg_{\alpha\gamma}$, and the sign convention is that if the wandering ghost line turns to its right with respect to its ongoing direction, like (b), the sliding diagram carries a plus sign. If it turns to its left like (c), the diagram carries a minus sign. In (f), two crosses are head to head on line-2. So the propagator of line-2 is cancelled.

- 1. 3g vertex: this is shown in Fig. 8.
- 2. 4q vertex:
 - (a) 4g vertex with one external line: if the crossed line is diagonal to the arrowed line, it is shown in Fig. 9. If the arrowed line is adjacent to the crossed line, it is shown in Fig. 10.
 - (b) 4q vertex with two diagonal external lines: it is shown in Fig. 11.
 - (c) 4q vertex with two adjacent external lines: it is shown in Fig. 12.
- 3. Ghost vertex with one external gluon and one internal gluon: it is shown in Fig. 13.

A.2 Cancellation relations

- 1. Cancellation relation involving ghost vertices with one external and one internal gluon line is shown in Fig. 14.
- 2. Cancellation relation involving the ghost vertex with two external gluon lines is shown in Fig. 15.
- 3. Cancellation relation involving the four gluon vertex with two diagonal external lines is shown in Fig. 16.
- 4. Cancellation relation involving the four gluon vertex with two adjacent external lines is shown in Fig. 17.

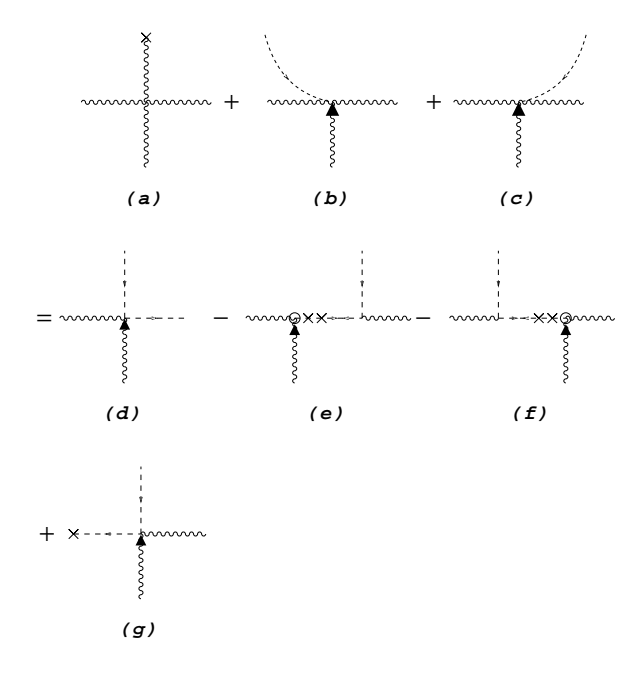


Figure 9: Divergence relation of a four-gluon vertex.

References

- [*] email address: feng@hep.physics.mcgill.ca
- [†] email address: lam@hep.physics.mcgill.ca
- [1] B.S. DeWitt, Phys. Rev. **162**, 1195, 1239 (1967); in *Dynamic theory of groups and fields* (Gordon and Breach, New York, 1965); G. 't Hooft, Nucl. Phys. **B62**, 444 (1973);
- [2] J.M. Cornwall, in *Proceeding of the French-American Seminar on Theoretical Aspects of Quantum Chromodynamics*, Marseille, France, 1981, edited by J.W. Dash (Centre de Physique Théorique, Marseille, 1982).
 - J.M. Cornwall, Phys. Rev. D 26, 1453 (1982).
 - J.M. Cornwall and J. Papavassiliou, Phys. Rev. D 40, 3474 (1989).
 - J. Papavassiliou, Phys. Rev. D 41, 3179 (1990); Phys. Rev. D 47, 4728 (1993).
 - G. Degrassi and A. Sirlin, Phys. Rev. D 46, 3104 (1992).
- [3] J. Papavassiliou and A. Pilaftsis, Phys. Rev. D 54, 5315 (1996).
- [4] A. Denner, G. Weiglein, and S. Dittmaiser, Phys. Lett, 333B, 420 (1994); S. Hashimoto,
 J. Kodaira, Y. Yasui, and K. Sasaki, Phys. Rev. D 50, 7066 (1994).
- [5] Y.J. Feng and C.S. Lam, Phys. Rev. D 53, 2115 (1996).
- [6] J.L. Gervais and A. Neveu, Nucl. Phys. **B46**, 381 (1972).
- [7] S. Leupold, hep-ph/9609222.

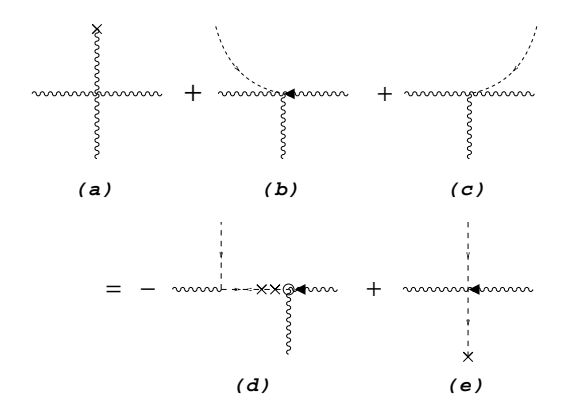


Figure 10: Another divergence relation of a four-gluon vertex.

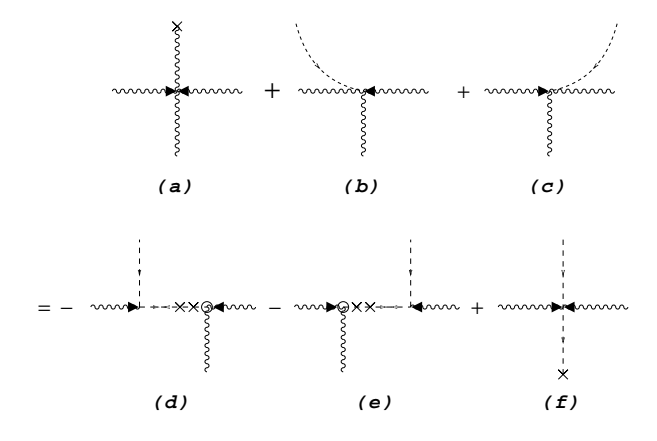


Figure 11: Divergence relation of a four-gluon vertex with arrowed lines.

- [8] M. Achhammer, U. Heinz, S. Leupold, U.A. Wiedemmann, hep-ph/9612033.
- [9] Y.J. Feng and C.S. Lam, in progress.
- [10] J. Paton and Chan Hong-Mo, Nucl. Phys. **B10**, 519 (1969).
- [11] R. Gastmans and Tai Tsun Wu, The Ubiquitous Photon Helicity Method for QED and QCD (Clarendon Pres, London, 1990);
 M.L. Mangano and S.J. Parke, Phys. Rep. 200, 301 (1991).
- [12] C.S. Lam, Nucl. Phys. B397, 143 (1993); Phys. Rev. D 48, 873 (1993); Can. J. Phys. 72, 415 (1994).
 Y.J. Feng and C.S. Lam, Phys. Rev. D 50, 7430 (1994).
- [13] L.F. Abbott, Nucl. Phys. **B185**, 189 (1981).

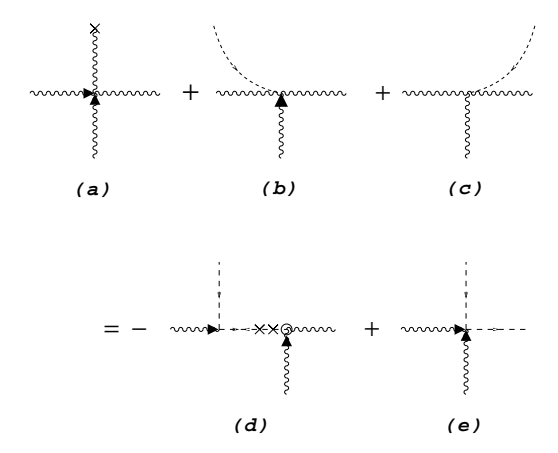


Figure 12: Another divergence relation of a four-gluon vertex with arrowed lines.

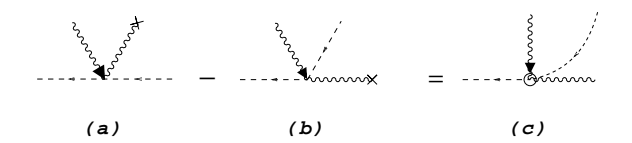


Figure 13: Divergence relation of a ghost vertex.



Figure 14: An identity (in the BF gauge).

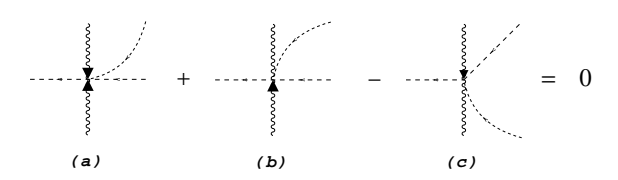


Figure 15: A cancellation relation.

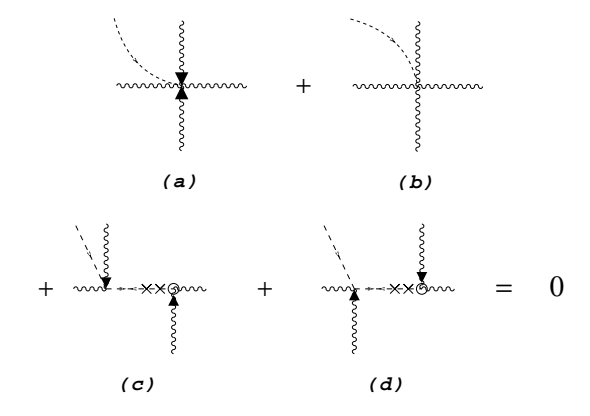


Figure 16: Another cancellation relation.

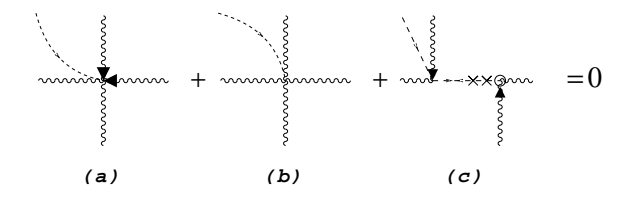


Figure 17: Yet another cancellation relation.